ORNL/TM-8496
Dist. Category UC-20 f

Contract No. W-7405-eng-26

ORNL/TM--8496

DE83 006359

FUSION ENERGY DIVISION

STELLARATOR PHYSICS EVALUATION STUDIES

J. F. Lyon

B. A. Carreras, R. A. Dory, S. P. Hirshman
J. H. Harris, L. Garcia, T. C. Jernigan
J. A. Rome, T. C. Hender, J. Sheffield

Fusion Energy Division

L. A. Charlton, H. R. Hicks, V. E. Lynch
R. H. Fowler, J. A. Holmes, B. F. Masden

UCC-ND Computer Sciences

D. L. Goodman, S. A. Hokin

Massachusetts Institute of Technology
Cambridge, Massachusetts 02139

Date Published - February 1983

Prepared by the
OAK RIDGE NATIONAL LABORATORY
Oak Ridge, Tennessee 37830
operated by
UNION CARBIDE CORPORATION
for the
DEPARTMENT OF ENERGY

CONTENTS

ABSTRACT

Stellarator/torsatron configurations with a wide range of parameters have been evaluated and compared in terms of their vacuum field topology, magnetohydrodynamic equilibrium and stability, and guiding center orbit confinement. The torsatron configurations are found to be the most suitable choice for a near-term physics experiment. The best of these configurations has an equilibrium beta limit of $\langle\beta\rangle \cong 5\%$ for a plasma aspect ratio of 7. The equilibrium limit can be increased to $\langle\beta\rangle \cong 8\%$ by doubling the aspect ratio. Modularization of the torsatron coils can be achieved in a practical way that retains all the physics properties of the configuration. The modularization introduces additional flexibility, which allows the realization of a larger variety of vacuum flux surface topologies. The feasibility of modularizing the coils and the reasonable physics parameters found for a configuration with moderate aspect ratio make torsatron configurations very attractive, both for physics experiments and for future fusion reactors.

1. INTRODUCTION

The key issue in stellarator design is finding a magnetic configuration that is optimal with respect to beta limits and low collisionality transport and extrapolates to a modular reactor. In this study, many stellarator/torsatron configurations were evaluated and compared using several different methods. The configurations studied were limited to modest coil aspect ratios (R/a_{coil} = 3.5-5) appropriate to a near-term experiment. The desired characteristics were magnetic surfaces with moderate aspect ratios ($R/\bar{a}$ = 6-12), average radius $\bar{a}$ = 20-30 cm, substantial rotational transform ($\iota_{max} \gtrsim 0.5$), moderate magnetic shear, and a modest well. Some of the stellarator configurations studied in this survey were: (1) $\ell = 2$ continuous-coil torsatrons, (2) $\ell = 2$ modular torsatrons, and (3) $\ell = 2$ modular stellarators. In all cases magnetic fields are calculated from filamentary windings ($\sim$200 elements each) with practical bend radii and coil separations, rather than from a simple model field expression. Replacement of a single filament by 4-8 filaments to simulate a finite conductor cross section reduces the average radius $\bar{a}$ of the last closed flux surface by $\lesssim$10%.

The properties evaluated in these studies were: (1) vacuum field flux surface topology and $\iota(r)$ profile, (2) guiding center orbit containment for thermal and fast ions, including electric fields, pitch angle scattering, and slowing down; and (3) magnetohydrodynamic (MHD) equilibrium and stability to low and high n modes. The MHD studies were done using three different methods: (a) averaged MHD equations based on the stellarator expansion [1], (b) the cylindrical, helically symmetric limit, and (c) full three-dimensional (3-D) calculations. These methods were applied in an iterative and interactive manner to optimize the configurations studied.

2. RESULTS OF CONFIGURATION EVALUATIONS

Among the magnetic configurations studied, the torsatrons (continuous and modular) are the most suitable for the given constraints. Moreover, the configuration properties (beta limits, particle confinement) were acceptable over a wide range of parameters (aspect ratio, number of toroidal periods m, winding modulation α). The best results were obtained with $\iota(0) \approx 0.3$, $\iota(\bar{a}) \approx 0.9$, and modest variation of $\int d\ell/B$ on flux surfaces (typically $\sim$15% at $r/\bar{a} \sim 0.7$). The maximum volume-average beta ($<\beta>$) values are due to equilibrium limits rather than stability limitations and are $<\beta> \cong 5\%$ for plasma aspect ratios $R/\bar{a} \approx 7$. This value can be increased to $<\beta> = 8\%$ by doubling the aspect ratio. Negligible fast ion losses occurred at B = 2 T for near-tangential 30-keV H^0 injection. Low ($\sim$1%) thermal ion losses occurred for collisionless 1-keV protons when plasma potentials $\sim$ 1 kV were included in the calculations.

The results for other configurations were not as favorable for a near-term base physics experiment, at least for the particular geometries studied. The modular stellarators studied had twisted toroidal field (TF) coils deformed sinusoidally in the toroidal direction [2,3]. Only simple, identical, circular, poloidally rotated coils were considered, where the jth coil (of N) was deformed toroidally by $\Delta_j(\theta) = d \sin[s\ell(\theta - \theta_j)]$, where $\ell = 2$ and $\theta_j = 2\pi mj/\ell N$. The harmonic enhancement factor s was greater than one in the region near the coil deflection nodal points to increase the rotational transform. The coil parameter ranges surveyed were m = 3-6 periods, N = 15-60 coils, and R/a_{coil} = 3-6. These configurations generally had decreasing $\iota(r)$ profiles with low shear and modest values of ι ($\sim$0.4-0.6) but relatively high rotational transform per period ($\iota/m \approx 0.1$). Magnetic surface quality at nonzero beta improves with increasing N/m (decreasing shear) and decreasing ι/m, but raising ι to find equilibria with $<\beta>$ above 1% leads to instabilities, probably due to the low shear of these configurations.

A reference m = 2 Heliac configuration [4] with a central toroidal ring conductor linking helically offset, circular TF coils was also studied. This coil geometry produces a helical magnetic axis, a magnetic

well with a depth that is relatively insensitive to coil aspect ratio, and intermediate rotational transform with low shear [$\iota(0) = 0.52$, $\iota(a) = 0.7$] but high transform per period ($\iota/m \approx 0.3\text{-}0.5$). This configuration, which shows favorable stability properties in the cylindrical limit [4], is very sensitive to toroidal effects for the aspect ratio considered here ($R/\bar{a} = 6$). The 3-D equilibrium calculations, which do not use a close-fitting conducting shell, indicate a low value for the limiting beta, $\langle\beta\rangle \lesssim 1\%$. With a close-fitting shell, this result can be improved to $\langle\beta\rangle \lesssim 3\%$. Better results have been obtained by doubling the aspect ratio.

3. TORSATRON OPTIMIZATION

The $\ell = 2$ torsatron configurations studied had helical coils with winding laws of the form $\phi = (\theta - \alpha \sin \theta)\ell/m$ with $R/a_{coil} = 3.5\text{-}5$, where ϕ is the toroidal angle and θ is the poloidal angle. Optimizing the vacuum field configuration for transform, vacuum magnetic well, and plasma radius gave $m = 10$, $\alpha = -0.2$, and $R/a_{coil} = 3.5$ with $\iota(0) = 0.15$, $\iota(a) = 0.7$, $\bar{a} = 32$ cm, and a 3.5% magnetic well. Equilibrium studies of this configuration using the Chodura-Schlüter code [5] gave an equilibrium beta limit $\langle\beta\rangle \approx 2.5\%$. The calculation is approximately flux-conserving (there is numerical dissipation, due to finite-grid effects, which allows island formation and magnetic surface breakup), and the net induced currents remain small. Depending on $\iota(r)$ and the pressure profile, $\langle\beta\rangle$ limits arise from equilibrium failure or large-scale instabilities. The equilibrium limitations are due to a large shift of the magnetic axis, which can cause the formation of an internal separatrix, to magnetic island formation, which can lead to destruction of magnetic surfaces, or to both. Bifurcation of the magnetic axis occurs for low $\iota(0)$ even for $\langle\beta\rangle < 1\%$. For $\iota(0) \gtrsim 0.3$, bifurcation occurs for higher values of β ($\langle\beta\rangle \sim 3\%$), and equilibria with good magnetic surfaces are found with $\langle\beta\rangle$ values above 4%. If $\iota(0) \gtrsim 0.5$, a $\langle\beta\rangle$ limit below 4% results from gross instability (loss of equilibrium) rather than excessive equilibrium shift. In the beta optimization from equilibrium considerations, the presence of a small magnetic well or hill in the vacuum configuration was less important than the value of $\iota(0)$. The best results ($\langle\beta\rangle \cong 5\%$) were obtained for $m = 12$, $\alpha = 0$, and $R/a_{coil} = 4.5$ with $\iota(0) = 0.3$, $\iota(\bar{a}) = 0.9$, $\bar{a} = 26$ cm, and a 1% magnetic well. The magnetic surfaces for this configuration at $\langle\beta\rangle = 4\%$ are shown in Fig. 1(a). Increasing the coil aspect ratio from 4.5 to 9 (plasma aspect ratio from 7 to 14) increased the equilibrium $\langle\beta\rangle$ limit to about 8%.

A parallel study of the equilibrium properties of the $\ell = 2$ torsatron configurations has been done using the stellarator expansion [1]. Equilibria have been calculated by requiring either zero net current on each flux surface or flux conservation. The latter method allows a more

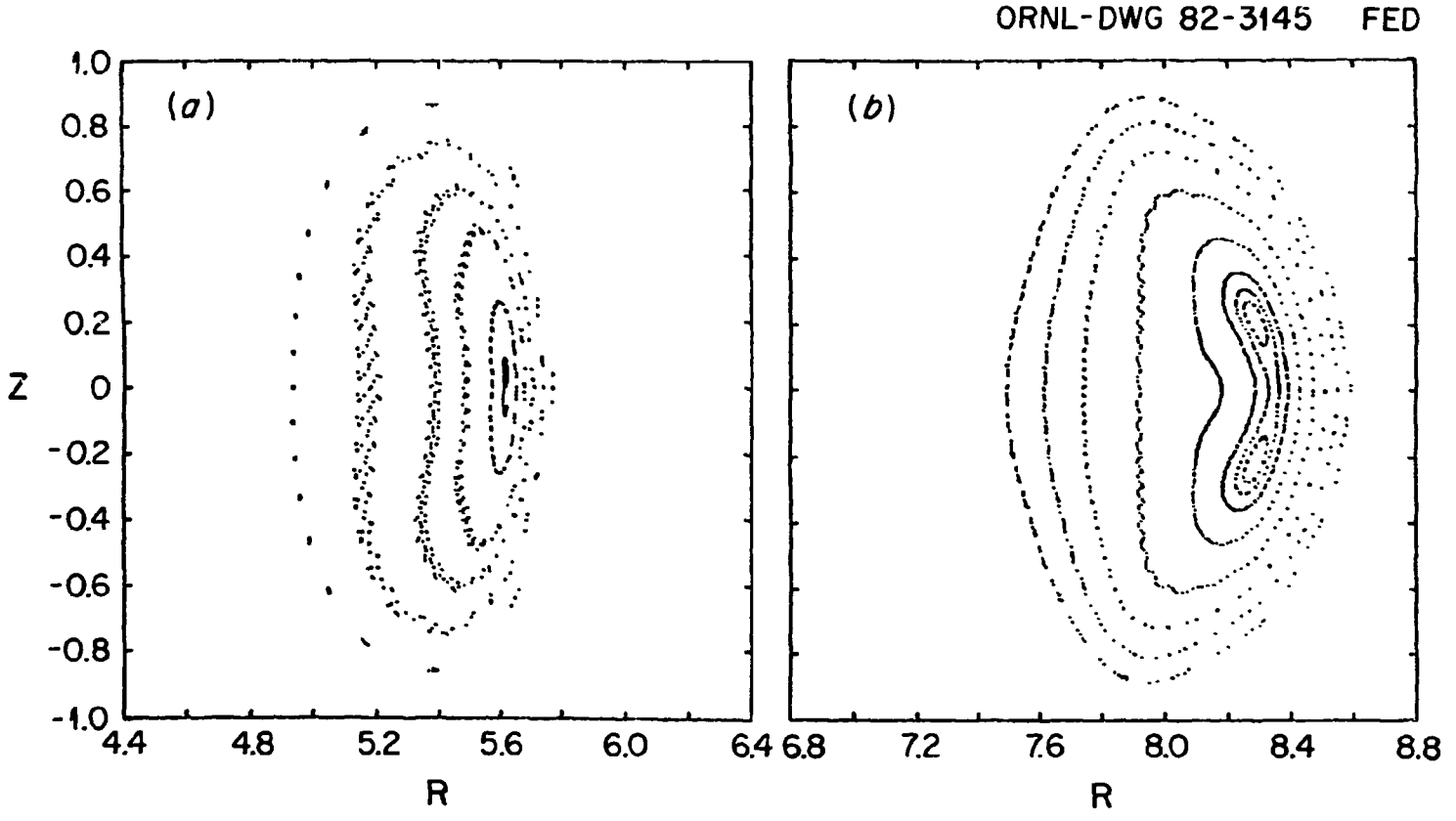

Fig. 1. Finite beta magnetic surfaces for (a) m = 12 torsatron with $\langle\beta\rangle$ = 4% and (b) m = 16 modular torsatron with $\langle\beta\rangle$ = 3%.

detailed comparison with the 3-D calculations described above. Figure 2 shows the calculated magnetic axis shift given by the different methods for the reference m = 12 continuous-coil torsatron. Pressure profile effects are also shown in this figure. Although the magnetic axis shift shows no dependence on the method of calculating the equilibrium, differences between flux conservation and zero net current constraints are contained in the β_c [= $2\iota^2(\bar{a})/A$] parameter. For the largest values of beta considered, there is significant deformation of the ι profile for the zero net current case. For a fixed value of $\langle\beta\rangle$ this method gives a larger shift than the flux-conserving calculation. The zero net current calculation is, however, overly pessimistic since realistic dissipation effects are not included. On the other hand, the presence of a small net current in the 3-D calculation, together with the numerically induced resistivity, can indicate an unrealistic breaking of magnetic surfaces. Therefore, in assessing a given configuration, we consider it very important to use these different methods.

Stability studies have been performed using the methods mentioned in Section 1. The calculations done for the cylindrical, helically symmetric limit using the HERA stability code [6,7] give very low beta limits. In particular, for the m = 12 continuous-coil torsatron configuration without toroidal curvature, the limiting value is $\langle\beta\rangle < 0.8\%$. The results are totally different when we use the reduced set of toroidal MHD equations [8] based on the stellarator expansion [1]. A modified version of the RST code [9] has been used for low n mode stability calculations to study stability for intermediate mode numbers ($1 \ll n \ll m$), and a ballooning limit of this set of equations has been derived. The results indicate no instability for equilibria up to $\langle\beta\rangle = 5\%$ (the limiting equilibrium). This indicates that toroidal effects are very important and that the magnetic well produced by the Shafranov shift is sufficient to stabilize these modes. A further test of these results has been done using the 3-D code to study the stability of the (2;1) mode for the cylindrical and toroidal configuration, with the same grid size used for both calculations. The cylindrical configuration shows a strong instability, but the toroidal one is stable. Therefore, the

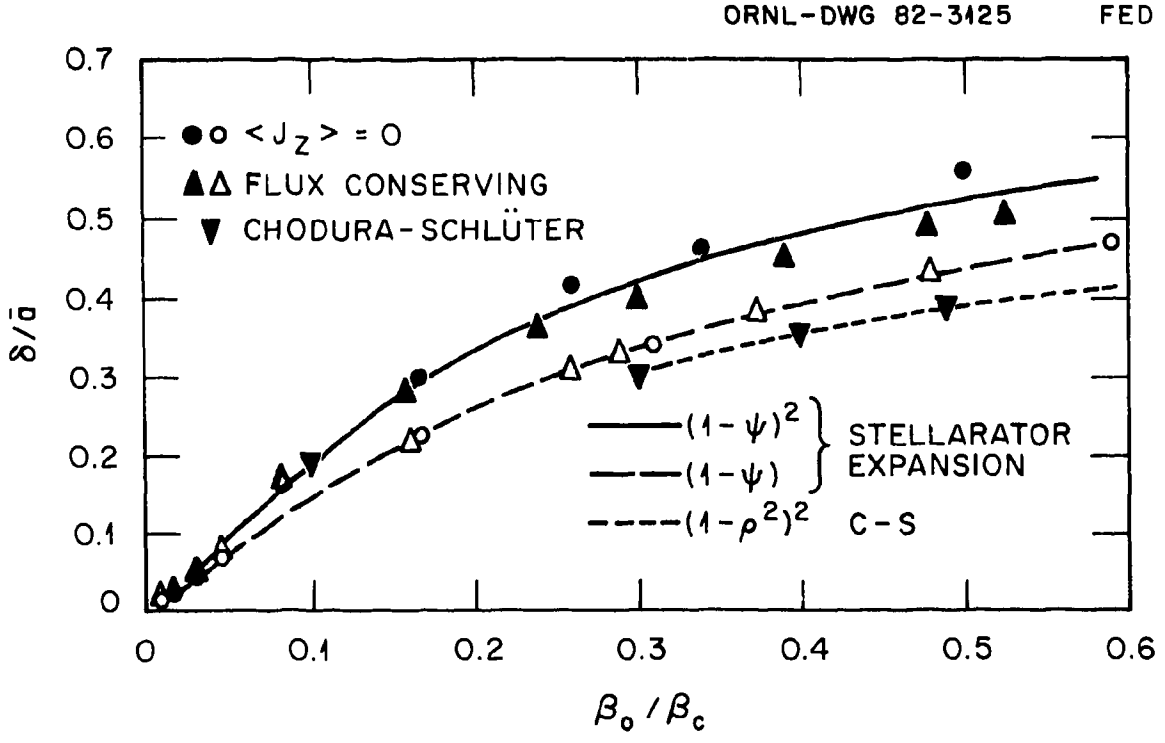

Fig. 2. Shift versus peak beta for m = 12 torsatron with $R/\bar{a} = 7$, $\iota(0) = 0.3$, $\iota(a) = 0.9$.

m = 12 torsatron configuration is found to be limited by equilibrium, rather than stability, considerations.

A new 3-D MHD code has been developed. It is similar to the Chodura-Schlüter code but uses vacuum flux surface coordinates [10] with a Fourier representation in the poloidal and toroidal directions. The equilibrium shifts obtained are in good agreement with the other codes. The m = 12 torsatron equilibria have also been tested for stability to the resonant low poloidal mode number modes using this code. No instability is found for $\langle\beta\rangle \lesssim 4\%$, which is in agreement with the results discussed above.

The main conclusion of these studies is that equilibrium and stability tend to give opposite restrictions on the configuration. An optimal configuration is one in which the magnetic axis shift with beta is small enough not to severely limit the equilibrium, but large enough to produce sufficient magnetic well to stabilize the ideal MHD modes. The m = 12 torsatron configuration fulfills these requirements.

4. MODULAR TORSATRONS

We have developed a technique for modularizing a torsatron that retains the good physics properties of that configuration. The modular torsatron, called the symmotron [11] (for symmetric modular torsatron), uses identical, nonrotated, helically deformed coils, one per field period, as shown in Fig. 3. The helical segments are connected by toroidally directed windbacks (the stray field of which must be compensated by toroidal ring coils not shown in Fig. 3), which also provide part of the vertical field needed for positioning the plasma. A variety of flux surface configurations can be produced by modulating the helical winding pitch (as in a conventional torsatron), winding the helix on a noncircular cross section, and varying the poloidal and radial location of the windback and compensating coils. For some choices of parameters, it is possible to obtain configurations with a helical magnetic axis. Figure 4 shows four extreme magnetic configurations obtained in this way. These configurations are far from optimum but are useful for examining the effects of internal flux surface topology, amount of $\int d\ell/B$ variation on a flux surface, etc.

Studies of MHD equilibrium like those done for continuous-coil torsatrons have been done for symmotrons. Figure 5 shows the magnetic axis shift for three modular torsatron configurations and the m = 12 continuous-coil torsatron shown in Fig. 1(a) as calculated by the Chodura-Schlüter code [5]. All three modular torsatrons (symmotrons) have triangular cross section tori, but cases A and B have the vertex at large R and case C has it at small R. Other differences are: case A has m = 16, $\iota(0) = 0.3$, $\iota(a) \approx 0.9$, and $R/\overline{a} = 9$; case B has m = 17, $\iota(0) \approx 0.3$, $\iota(a) \approx 0.9$, and $R/\overline{a} = 9$; and case C has m = 17, $\iota(0) = 0.1$, $\iota(a) \approx 0.85$, and $R/\overline{a} = 8$.

The main difference among cases A, B, and C in Fig. 5 is the reduction from case B to A to C in $\int d\ell/B$ variation on a flux surface, which is also correlated with reduced guiding center orbit losses. For example, case C has a direct loss of 30-keV collisionless orbits of $\sim$7% versus $\sim$20% for case B or the m = 12 torsatron, whereas a configuration with a larger $\int d\ell/B$ variation [Fig. 4(d)] has a much larger direct

ORNL-DWG 82-3146 FED

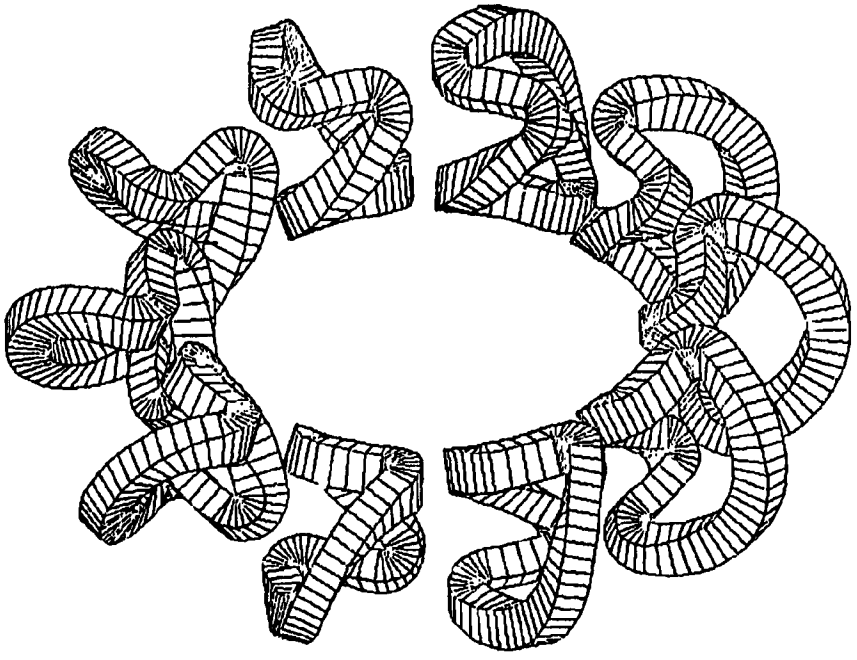

Fig. 3. Symmotron scheme for modularization of m = 10 torsatron. Circular cross-section torus with windbacks on the small R side is shown.

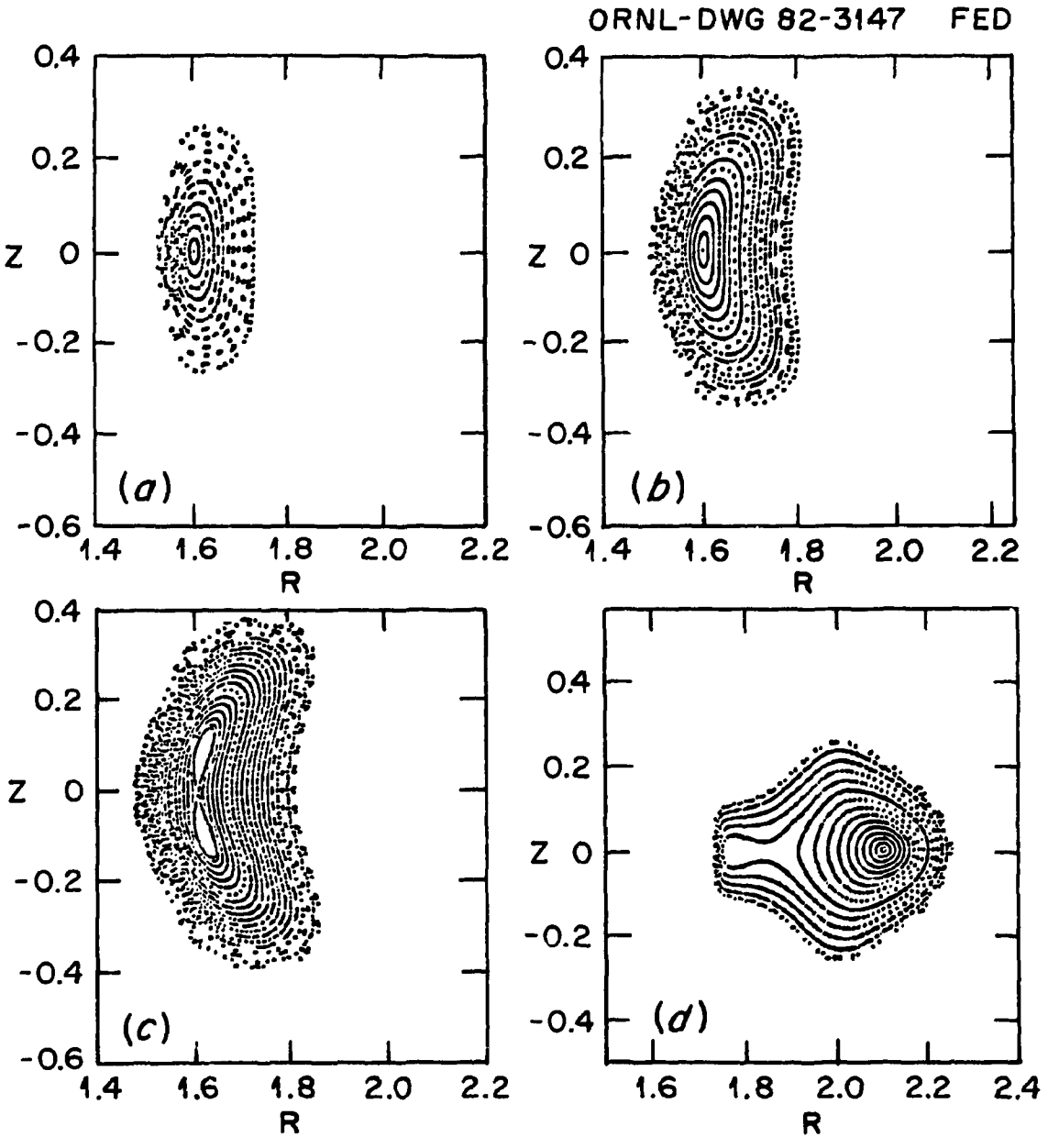

Fig. 4. Flux surfaces for four extreme (nonoptimal) symmotron configurations.

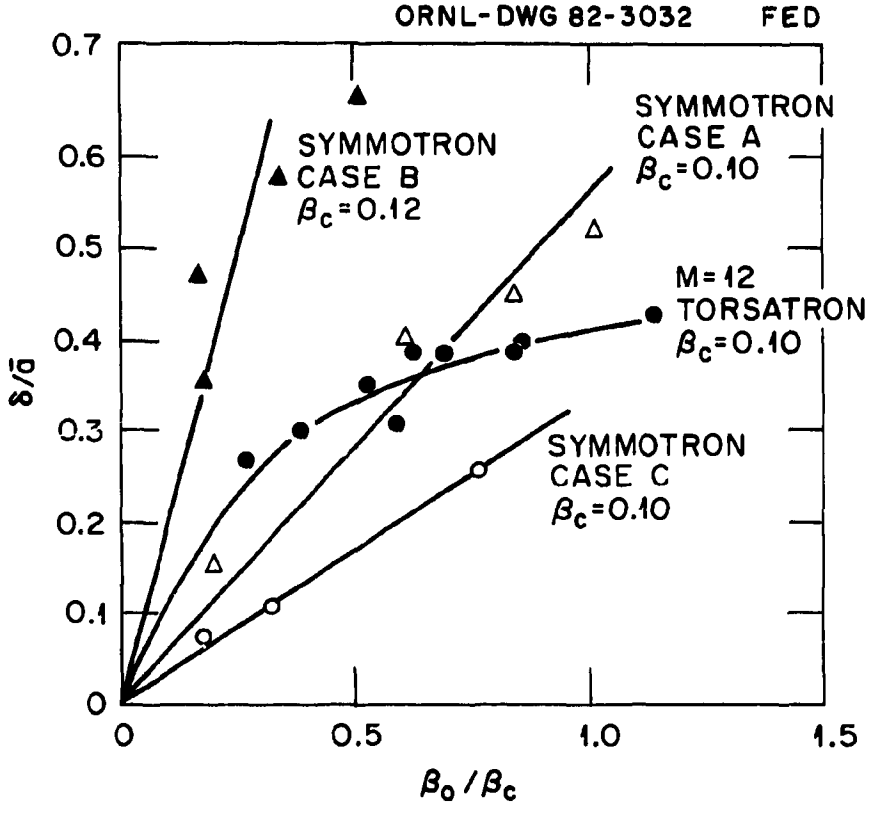

Fig. 5. Shift versus peak beta for torsatron and symmotron configurations.

30-keV orbit loss (∿60%). In general, collisionless guiding center orbit losses are similar for different configurations [e.g., ∿30-40% for 30-keV H^+ in 2-T fields for the configurations shown in Fig. 4(a)-(c)] and hence are not as sensitive an indicator of configuration quality as is the equilibrium beta limit. The actual orbit losses for a given configuration would be smaller, however, because of the effects of potential and collisions.

The moderate-shift modular torsatron configuration (case B of Fig. 5) has m = 16, α = 0, and a triangular cross-section torus with the vertex at small R. Figure 1(b) shows the magnetic surfaces for a $\langle\beta\rangle$ = 3% equilibrium for this configuration, which are similar to the m = 12 torsatron surfaces shown in Fig. 1(a). The values of $\iota(0)$, $\iota(a)$, and the equilibrium beta limit ($\langle\beta\rangle$ = 4-5%) are the same for the two configurations, but the modular torsatron has a slightly smaller average radius of the last closed flux surface (∿15% smaller for equal R), principally due to the perturbation caused by the windback and compensating windings. The particle confinement properties of the two configurations are also very similar, and it is clear from our studies that the modularization per se has little effect on orbit containment.

The value of the vertical field B_v needed for horizontally positioning the magnetic axis is a useful variable in optimizing the nonzero beta equilibrium quality. The optimum value of B_v for $\langle\beta\rangle \neq 0$ is different from that for $\langle\beta\rangle = 0$, as might be expected, but the final equilibrium flux surface configuration attained for a given $\langle\beta\rangle$ also depends on whether the additional B_v is applied at the start of the relaxation toward an equilibrium or after an initial equilibrium is attained if magnetic reconnection is allowed.

Modular torsatrons thus prove to be as good as continuous-coil torsatrons from the standpoint of physics properties. Their only drawback is that they have average plasma radii that are 10-20% smaller than those of an equivalent continuous-coil torsatron. This poses no problem in a reactor, where the plasma volume utilization must be reduced somewhat to accommodate the blanket and shield, but it is important for a physics experiment, in which the coil size must be minimized for a fixed plasma radius to reduce costs.

5. GUIDING CENTER ORBIT STUDIES

Proper treatment of guiding center orbits is required to evaluate the extent of loss regions, fast ion heating efficiency, and particle and energy transport. This can be done as accurately as required (typically 0.1-1.0%) by using a Fourier representation of the magnetic field in field line coordinates [10]. Following guiding center orbits in field line coordinates is an order of magnitude faster than using the Biot-Savart law in real space, and because the extraneous helical motion of the field lines is eliminated, the deviation of the orbit from a flux surface (ψ = constant) is evident. Figure 6 shows two typical collisionless 30-keV proton orbits in a 2-T field in ψ-θ coordinates, (a) a co-passing orbit and (b) a helically trapped orbit.

Collisionless orbit losses are dominated by trapped particles and in particular by those transitional particles that change from passing to helically trapped. In order to evaluate direct collisionless orbit losses, $\sim$100 ions randomly distributed in $v_{\|}/v$ and ψ, θ, ϕ are followed for $\sim$20 toroidal or $\sim$3 poloidal transits. Direct losses of 30-keV protons in 2-T fields are $\sim$20% for $|v_{\|}/v| < 0.5$, but only $\sim$1-4% for $|v_{\|}/v| > 0.5$, as would occur for quasi-tangential neutral beam injection. Much larger losses (factor of $\sim$3) occur for configurations with horizontally bifurcated magnetic axes and large $\int d\ell/B$ variations on a flux surface, while much smaller losses (factor of $\sim$3) occur for configurations with small $\int d\ell/B$ variations. However, optimal containment occurs before the minimum in $\int d\ell/B$ is reached. Removing the toroidally symmetric (n = 0) harmonics from the field representation yields omnigenous orbits for circulating and banana-trapped particles. For protons below 5 keV, a 1-kV potential generally has more effect on losses than magnetic configuration parameters. In these cases $\sim$1% of 1-keV collisionless protons are directly lost, and the average maximum deviation of an orbit from its average flux surface $\bar{\psi}$ is $\Delta\psi \sim 1/15(\psi_{wall} - \bar{\psi})$, where $0 < \psi < 1$.

Accurate loss estimates for quasi-tangential neutral beam injection cases are obtained by Monte Carlo beam deposition along a realistic beam trajectory, transformation of the beam ion birth points to field line

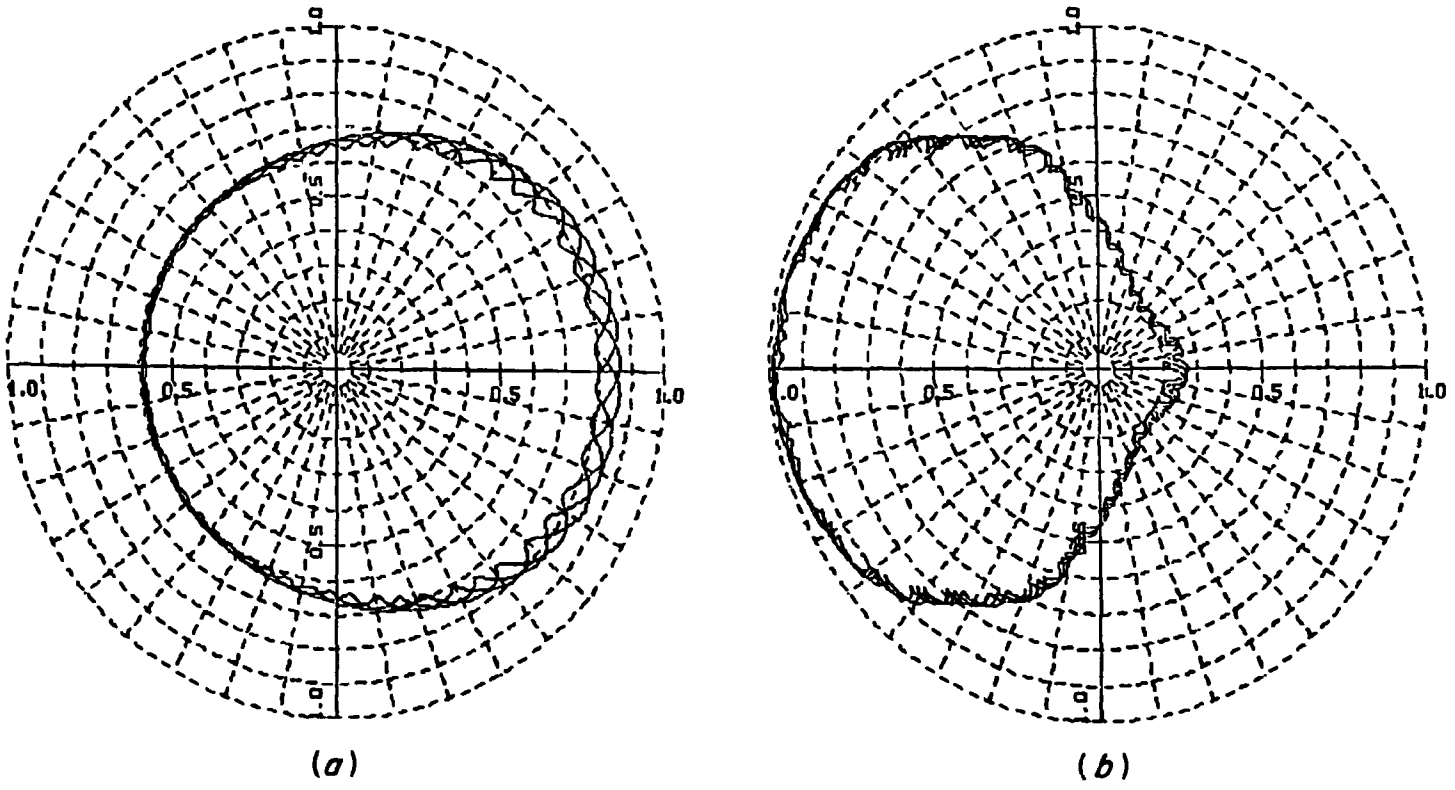

Fig. 6. 30-keV collisionless orbits in a 2-T field in an m = 10 torsatron for (a) a co-passing proton and (b) a trapped proton.

coordinates, and orbit following in field line coordinates with analytic slowing down and random pitch angle scattering. For quasi-tangential, 30-keV, H^0 neutral beam injection in a 2-T field, with $T_e(\psi) = (1 - \psi)$ keV and $n_e(\psi) = (1 - \psi)10^{14}$ cm^{-3}, no significant energy loss to the wall occurs as the beam slows down on the background plasma, even in the absence of an electric field. This calculation is not sensitive to configuration details for the cases studied.

A potentially sensitive indicator of configuration quality is that of thermal ion confinement. Estimates of confinement times for thermal particles are obtained in the presence of pitch angle scattering, using a Monte Carlo method similar to that employed by Wobig [12]. Rather than calculating a spread in $\overline{\psi}$ of an orbit to obtain a diffusion coefficient, the equilibrium loss rate (to the wall) of ions born on a given flux surface ψ' is calculated. Lost ions are replaced at ψ' but with random θ, ϕ, and $v_{\|}/v$. The mean time for loss to the wall from a given flux surface ψ' decreases exponentially with ψ' and increases rapidly with electric field strength. For a parabolic potential $\Phi(\psi)$, only ions born at $\psi \gtrsim 0.9$ are lost for $\Phi(0) < -T_e(0)$. Ions inside $\psi \sim 0.9$ are electrostatically confined and are not lost. The large excursions in ψ that eventually lead to loss to the wall result from orbits changing from passing to trapped and not from a diffusive process. When the bulk of the plasma is in the plateau regime, the trapped particle orbits that would be lost collisionlessly are interrupted by collisions, while the contained passing particles are relatively unaffected.

Guiding center orbits in the finite beta equilibria obtained from the Chodura-Schlüter code are now being studied for the first time. If $\int d\ell/B$ is really constant on the finite beta flux surfaces, the orbit containment and transport might be much better than in the vacuum state.

6. CONCLUSIONS

Moderate-shear torsatrons (either continuous or modular coils) give equilibrium beta limits $<\beta> \sim 5\%$ and acceptable orbit confinement for a near-term experiment. Since both the beta limit and the orbit confinement improve with an increase in aspect ratio toward reactor dimensions, and since torsatrons can be successfully modularized, this configuration looks attractive on a reactor scale.

ACKNOWLEDGMENTS

The authors gratefully acknowledge useful discussions with J. D. Cullen, T. K. Chu, P. R. Garabedian, H. Weitzner, and S. Yoshikawa and the support of M. J. Saltmarsh, O. B. Morgan, and M. W. Rosenthal.

REFERENCES

[1] GREENE, J. M., JOHNSON, J. L., Phys. Fluids 4 (1961) 875.

[2] REHKER, S., WOBIG, H., Proc. 7th Symp. on Fusion Technology (Grenoble, 1972) 345.

[3] CHU, T.K., FURTH, H. P., JOHNSON, J. L., LUDESCHER, C., WEIMER, K. E., IEEE Trans. Plasma Sci. 9 (1981) 228.

[4] YOSHIKAWA, S., CHU, T. K., private communication (1982).

[5] CHODURA, R., SCHLÜTER, A., J. Comput. Phys. 41 (1981) 68.

[6] CHODURA, R., GRUBER, R., HERRNEGGER, F., KERNER, W., SCHNEIDER, W., TROYON, F., Plasma Physics and Controlled Nuclear Fusion Research (Proc. 8th Int. Conf. Brussels, 1980) Vol. I, IAEA, Vienna (1980) 813.

[7] LORTZ, D., NÜHRENBERG, J., Plasma Physics and Controlled Nuclear Fusion Research (Proc. 7th Int. Conf. Innsbruck, 1978) Vol. II, IAEA, Vienna (1979) 309.

[8] STRAUSS, H. R., Plasma Phys. 22 (1980) 733.

[9] LYNCH, V. E., CARRERAS, B. A., HICKS, H. R., HOLMES, J. A., GARCIA, L., Comput. Phys. Commun. 24 (1981) 465.

[10] BOOZER, A. H., Princeton Plasma Physics Laboratory Rep. PPPL-1775 (1981).

[11] ROME, J. A., Proc. 3rd Stellarator Study Workshop (New York, 1982) New York University, New York (1982) 223.

[12] WOBIG, H., private communication (1982).